Global Flow Measurement Workshop
22 - 24 October 2024

Technical Paper

CO2 Gas meter performance for CCUS applications

Wan Adrie, Petronas, Malaysia (JIP Technical Comittee Chair)
Dennis van Putten, DNV, Netherlands
Mohammed Al Saleem, DNV, Netherlands

1 INTRODUCTION

As global decarbonization efforts gain momentum, the transport of CO_2 assumes a pivotal role in facilitating Carbon Capture, Utilization, and Storage (CCUS). Beyond natural gas systems, accurate measurement and subsequent billing for CCUS are essential to demonstrate compliance with national and international emissions-reduction regulations, including the EU Emission Trading System (ETS).

Worldwide regulations are rapidly evolving, and stringent measurement accuracy requirements for flow metering are anticipated to fall within the range of 1% to 2.5% for mass flow, regardless of the thermodynamic phase. These requirements apply universally, imposing new challenges on flow metering technology and systems.

In the recently executed Joint Industry Project (JIP CO2MET Gas), DNV collaborated with 24 industry partners to tackle the challenges associated with gas CO_2 measurements. At last years workshop part of this JIP was presented [**10**], focusing on the application of flow metering in transport networks. The JIP also involved an extensive testing campaign, of which the results will be presented in this work. The testing focused on two main application scenarios: onshore CO_2 gas transport (medium pressure/medium temperature) and vapor return during liquid ship on/offloading (low pressure/low temperature). A diverse range of metering technologies—Coriolis, ultrasonic, turbine, vortex, Venturi, and V-cone meters—were rigorously evaluated.

2 OPERATOR PERSPECTIVE

The push for decarbonization has let to many energy organizations pledging to be carbon neutral in the near future, some, as early as 2050. For example, the Hydrocarbon and Gas Technical Comittee under Department of Standards, Malaysia and many other nations globally have intensified efforts to adhere to aspirations by the recent COP 28. While we speak, PETRONAS is in the middle of converting its mature wells into carbon storage facilites.

The emergance of CCS as a revenue stream will translate to the fiscalization of the CO_2 metering at various points of the value chain. Carbon taxation will make that a certainty. We now face a race against time to technically arrive to a practicable range for the expected uncertainty for CO_2 metering.

South East Asia is now leading the charge for CCS facilities, specifcally in Malaysia where theres are 3 CO_2 hubs, along with CCS are being developed. The PETRONAS flagship Kasawari facility is almost ready (see Figure 3-1), located offshore Sarawak, Malaysia is the world's largest offshore CCS; and PTTEPs Lang Lebah CCS developement is hot on its heels.

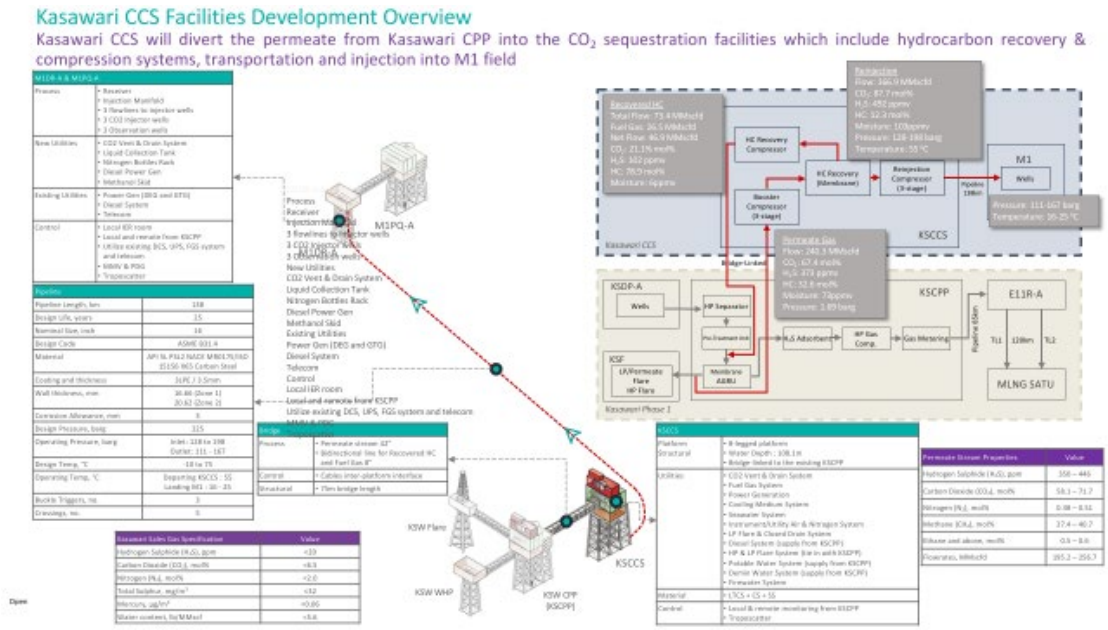

Figure 2-1 : Kasawari CCS facility overview

Our participation in the DNV JIP, from an operators perspective; is crucial to the development of the facility as the key findings and outcome of focused discussions with fellow practitioners and experts will result in realizing an efficient CCS facility.

During the 2021 edition of the GFMW, PETRONAS was involved in discussions with experts from DNV on the possibiliy of being part of the then propsed JIP, and hoping to play an active role in it. That has now been partially realized as theres still quite a bit to do as we have only managed to accomplish the gas portion for now. In the main, we will continue to participate in incoming JIPs, especially the inbound CO_2 liquid and dense phase metrology, the CO_2 quality measurerment, and also the H2Met as well.

The technical comittee, together with the voting members of the quoroum, is organizing a two day workshop, where hopefully the results which we will be discussing later will be central to the development of inbound international standards on CO_2 metrology.

3 REFERENCE SYSTEM

The reference system of the DNV facility used for gaseous CO_2 tests is shown in Figure 3-1. It consists of a part with two lines of 4" and 6" with a Coriolis and turbine meter in series. These lines can be used in parallel or separately by using the block valves. The 4" line contains an Emerson Micromotion CMF200 and an FMG FMT-M400, the 6" line contains an Emerson Micromotion CMF300 and an FMG FMT-M1000. Downstream this section, a 6-fold sonic nozzle system is installed. Each of the nozzles can be used by opening the block valves.

For the flow technologies that require additional physical property input (e.g. density for the turbine meter) the GERG-2008 equation of state [**1**], [**6**] was used.

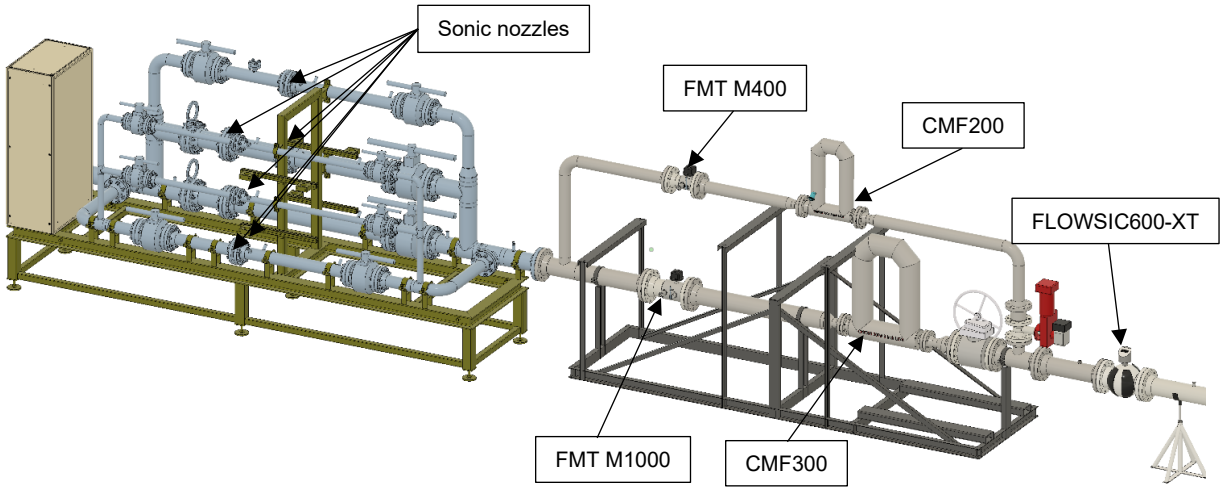

Figure 3-1 : Gas reference system for CO_2 applications at DNV facility Groningen

The system benefits from the three different measurement technologies which all have a different traceability chain. The Coriolis meters are calibrated on atmospheric water (traceability to liquid mass via VSL water facility) and theoretical compensation methods for pressure and compressibility are applied for the usage on high pressure gas. The turbine meters are compensated for the bearing friction by means of the PTB turbine meter model and calibrated on natural gas (traceability to EUREGA harmonized cubic meter via Force and DNV gas facilities). The sonic nozzles are traceable to the meter via the dimensional measurements of the nozzle throat and via the PTB atmospheric air flow calibration facility. A more elaborate description and its traceability is provided in [**7**].

Upstream the reference system a SICK FLOWSIC600-XT is added to verify the gas composition by means of the speed of sound, see for more details section 3.3. The ultrasonic flow meter also provides the volumetric flow rate, which is used for verification but is not used in the reference system for mass flow determination.

3.1 Turbine meter usage and corrections

The PTB turbine meter model is based on the combined effect of fluid dynamics and rotational mechanics in which the error of the turbine meter can be written as:

$$\epsilon_{\mathrm{T}} = g(\mathrm{Re}) + \frac{b_0}{\rho Q^2} + \frac{b_1(T)}{\rho Q}(1 + \epsilon_{\mathrm{T}}) + c_p \frac{\rho Q^2}{p}, \qquad (1)$$

where Q is in m³/s, p is the pressure in Pa, and ρ is the mass density. The second and third term on the right-hand-side are the static and dynamic bearing friction corrections that become dominant at low flow rates (b_0 and $b_1(T)$ are the static and dynamic bearing friction coefficients, respectively). The last term is related to the fact that the temperature at the turbine blades is different from the temperature at the measurement location and become dominant at high flow

rates. More formally, the last term can be rewritten which shows it is proportional to $c_p \kappa \mathrm{Ma}^2$, with κ the isentropic expansion coefficient, Ma the Mach number and c_p the proportionality constant. Hence, this term becomes dominant at high Mach numbers. Once compensated for these effects a pure Reynolds behaviour is obtained, which can be represented by a polynomial function of the form:

$$g(\mathrm{Re}) = \sum_{j=0}^{n} a_j [\log(\mathrm{Re}/\mathrm{Re_c})]^j. \quad (2)$$

This Reynolds curve is transferable between different gases, i.e. the Reynolds calibration that is performed under natural gas and air can be used for the CO_2-rich gases. Since a change in temperature can change the lubrication properties of the bearings, a temperature dependent dynamic bearing friction coefficient is implemented based on the viscosity datasheet of the lubricant. The model used for predicting the bearing friction properties is based on the exponential behaviour as function of temperature and only affects the dynamic bearing friction coefficient:

$$b_1(T) = b_1(15) \cdot e^{-d(T-15)} \quad (3)$$

The parameter d is determined from the viscosity datasheet of the lubrication oil (Aeroshell fluid 12). The increased bearing friction is verified by means of the spin down curves and show a good agreement for the 4" turbine meter.

The coefficients for the PTB turbine meter model used during the CO_2MET test are listed in Table 1.

Table 1 : PTB turbine meter coefficients for the CO_2MET gas test

PTB coefficient	FMG DN100	FMG DN150
a_0	0.3000	-0.0865
a_1	0.5879	-0.4871
a_2	-0.1382	0.3320
a_3	-0.5792	-0.1194
a_4	0.0664	0.0118
b_0	$-1.73 \cdot 10^{-5}$	$-2.97 \cdot 10^{-4}$
b_1(T=15)	$-2.02 \cdot 10^{-2}$	$-2.67 \cdot 10^{-2}$
d	$4.614 \cdot 10^{-2}$	$4.614 \cdot 10^{-2}$
c_p	$-1.6 \cdot 10^{6}$	$-1.8 \cdot 10^{5}$
Re_c	$3 \cdot 10^{5}$	$4 \cdot 10^{5}$

3.2 Coriolis meter usage and corrections

The Coriolis meters are traceable to the water standard at (nearly) atmospheric and need compensation for the pressure and the compressibility of the gas medium. The pressure correction has its origin in the change in shape of the tubes and is well-known. The corrections are published in the Emerson PDS [**3**] and are of the form:

$$\epsilon_p = 1 + f \cdot (p - p_0), \quad (4)$$

where $p_0 = 2\mathrm{bara}$ is the calibration pressure and f is the meter dependent correction factor. A similar correction is available for the density measurement. The density is also corrected with a constant factor based on the experience of DNV on a range of pressures and gas compositions. The density measurement is not used as an input for the reference system and used for verification purposes only.

Next to the pressure correction, also a speed of sound correction is applied. This correction is not stated in the PDS and is based on the Hemp and Kutin model [**5**]:

$$\epsilon_c = 1 + 0.5\left(\frac{\omega R}{c}\right)^2, \tag{5}$$

where ω and R are the angular frequency and the radius of the Coriolis tubes.

More recently, a Mach number dependence was investigated in [**2**], however, this term becomes dominant at tube Mach numbers of $\mathrm{Ma} > 0.2$ which will not be reached in the JIP CO_2MET Gas.

3.3 Ultrasonic meter usage and corrections

The SICK ultrasonic meter was calibrated under ISO17025 on natural gas with traceability to the EUREGA harmonized standard cube at the DNV gas calibration facility. Calibrations were carried out on a range of pressures to cover the Reynolds range of the JIP. The usage of the meter under different gases enforced the use of only the two centre paths of the meter. Therefore, the raw path velocity signals (corrected for pressure and temperature effects) were used to determine the volume flow rate (using a pressure and temperature compensated cross-sectional area of the meter). The Reynolds correction curve is based on this calculated volume flow rate.

The measured speed of sound of the SICK ultrasonic meter is used to verify the gas composition from the GC. Based on the provided gas composition, the speed of sound is calculated via the equation of state for the temperature and pressure at the SICK ultrasonic meter. The sensitivity of the speed of sound for changes in the composition depends on the specific gas component and therefore can only be used to verify the ratio between gas component with sufficiently different speed of sounds. In the CO_2MET JIP, the dominant ratio is CO_2-to-rest components and differences of up to 0.1 %mol on CO_2 can be detected.

Special care needs to be taken for low-pressure CO_2 tests since the speed of sound becomes frequency dependent, see [**9**]. The frequency of the SICK ultrasonic meter (80kHz) has been reduced to minimize this effect.

Moreover, the speed of sound is used as an additional density verification as:

$$\rho = \frac{p\kappa}{c^2}. \tag{6}$$

This circumvents the conversion to a molar mass and can be regarded as an accurate density estimator, since κ is a mild function of composition and both pressure and speed of sound can be measured with high accuracy, see [**4**].

4 TEST SECTION DESIGN AND PERFORMANCE EVALUATION

The JIP CO_2MET Gas test was divided among two main applications: onshore pipeline transport (medium-temperature/high-pressure) and shipping, (ship loading/unloading), (low-temperature/low-pressure). These test applications required a dedicated test setup and matrix and were therefore separately elaborated.

The test conditions that were achievable during the JIP are limited to the facility capabilities:

- Pressure: 7 – 33 bara
- Temperature:
  - 5 – 35 °C in normal configuration, i.e. without additional cooling equipment
  - -40 – 35 °C with additional cooling equipment.
- Any pressure-temperature combination should result in a pure gas phase for the gas mixture under test. With the use of the sonic nozzles also single-phase conditions are required at nozzle throat conditions.
- Maximum flow: 1000 m^3/h at suction side of pump, i.e. at 10 % relative pressure drop over the test facility, the flow will reduce 10 % at the discharge side of the pump.
- Any blend of gases, except for hazardous components like H_2S.

For each test condition, a nitrogen baseline test was performed to check the Meter Under Test (MUT) configuration and the DNV reference system. This baseline test was meant as a system verification and was not used to adjust the MUTs.

4.1 Medium temperature test (onshore pipeline transport)

For the medium temperature test, a test setup was designed according to the specification of the manufacturers. This setup is depicted in Figure 4-1, where the green arrows indicate the flow direction. The test consisted of two parallel 4” test lines to minimize the total pressure drop over the test section. The lines were blocked-in by means of two valves and bleeding the section in between (double block and bleed (DBB) configuration).

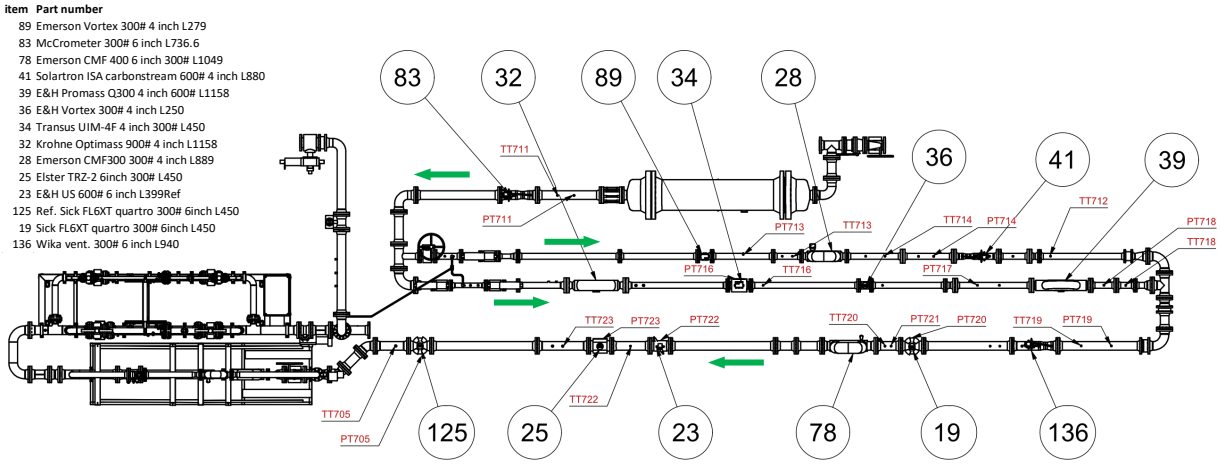

Figure 4-1 : Test setup for medium temperature test (onshore pipeline transport)

4.2 Low temperature tests (medium/low-pressure shipping)

For the low temperature tests corresponding to the vapor return line application of medium/low-pressure shipping, a test setup was designed and is provided in Figure 4-2. Also, this test setup consisted of two parallel test line to minimize the total pressure drop over the test. For the low temperature cases, no DBB configuration was present, and the bypassed test line will be reconstructed during the test and blinded off. The test setup including the reference system was insulated in a cold-box to prevent ice formation on the test section and improve cooling efficiency during the test.

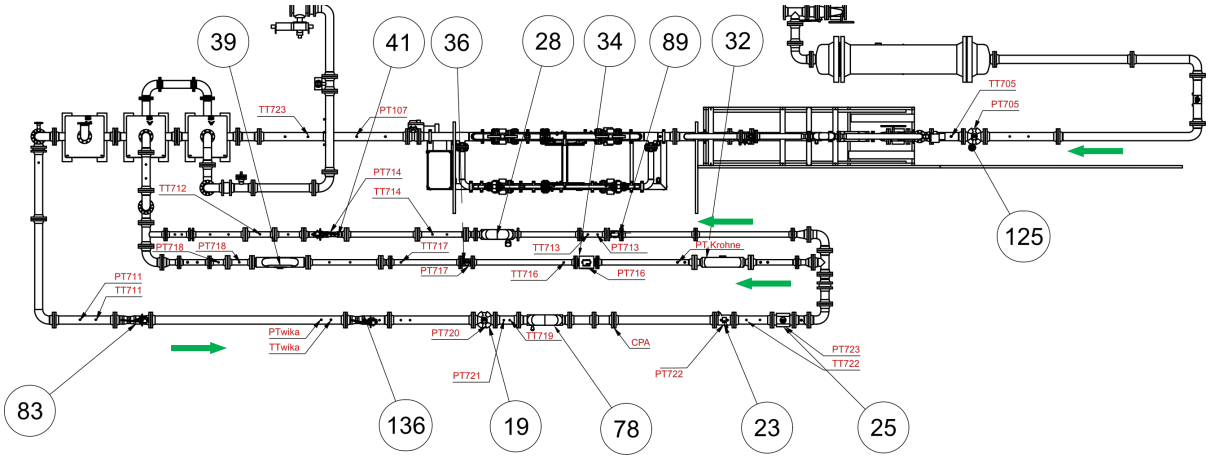

Figure 4-2 : Test setup for low temperature test (medium- & low-pressure shipping)

The two test setups in the DNV flow facility are show in figure Figure 4-3 with the medium temperature case on the left and the test section for the low temperature case on the right (test section still under construction showing the main test line).

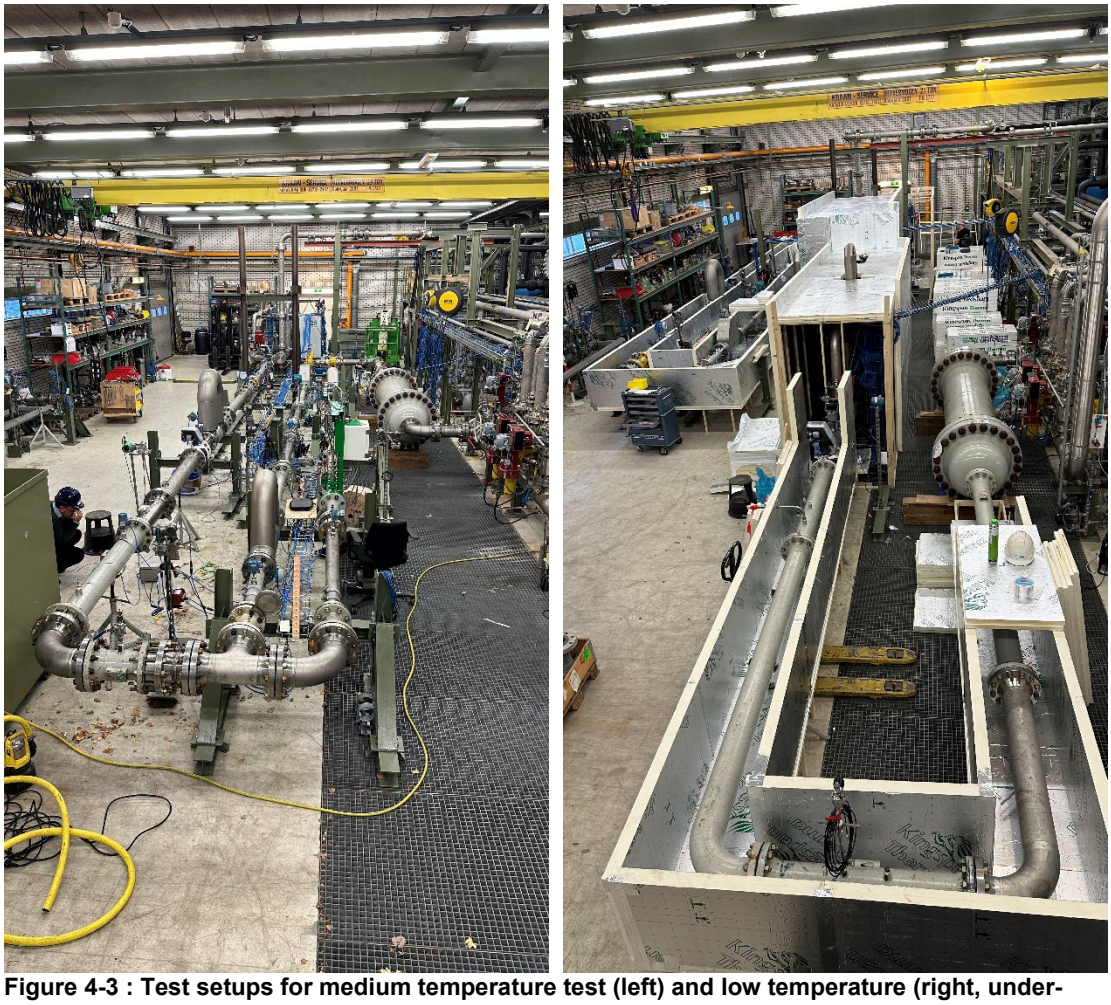

Figure 4-3 : Test setups for medium temperature test (left) and low temperature (right, under-construction)

4.2 Performance evaluation method

The MUT data from the test campaign was analysed and compared to the results provided by the reference system. The performance evaluation was based on the relative deviation of the mass flow of the MUT, denoted by m_i^{MUT}, from the mass flow of the reference system, denoted by m_i^{REF} (calculated by a weighted average of the three-fold reference system), defined as:

$$\varepsilon_i = \frac{m_i^{MUT} - m_i^{REF}}{m_i^{REF}}. \quad (7)$$

For volume-based meters, DNV calculated the density at the MUT based on the reference pressure and temperature and the same equation of state (GERG-2008) as used for the reference system.

For the performance evaluation, a similar process as defined in the OIML 137-1/2 [**8**] will be followed. In the OIML, both the Maximum Permissible Error (MPE) and the Weighted Mean Error (WME) will be used to determine the accuracy class a flow meter complies with. The MPE depends on the operational range of the flow meter and makes a distinction between the maximum flow rate Q_{max}, the minimum flow rate, Q_{min}, and the transitional flow rate Q_t. The performance assessment should be based on test points between Q_{min} and Q_{max}, whereas the transitional flow rate makes a distinction in the lower/upper region of operation. This distinction is made for the MPE which is different for both regions, see Table 1.

Table 1 : MPE specification from OIML 137 for type evaluation and initial verification

	Accuracy class		
Flow rate range	**0.5**	**1**	**1.5**
$Q_{min} < Q_i < Q_t$	±1 %	±2 %	±3 %
$Q_t \leq Q_i \leq Q_{max}$	±0.5 %	±1 %	±1.5 %

If a meter does not have a specified Q_t, the OIML offers the guideline as a minimum requirement as stipulated in Table 2. Most meters within the JIP test campaign fall under the second category ($5 \leq Q_{max}/Q_{min} < 50$) and therefore Q_t should at least be 1/5 of Q_{max}.

Table 2 : Flow meter characteristics according to OIML 137

Q_{max}/Q_{min}	Q_{max}/Q_t
≥50	≥10
≥5 and <50	≥5

It is noted that for a qualification test of accuracy class 0.5, the facility uncertainty should formally be lower than one-third of the MPE. As will be explained in section 5.1, this cannot be achieved by the DNV test facility and therefore only meters of class 1 can be qualified. It is emphasized that attaining the one-third criterion is a challenge for any (CO_2) gas calibration facility.

The Weighted Means Error (WME) is determined by flow weighting of the relative deviations:

$$\mathrm{WME} = \frac{\sum_{i=1}^{N} k_i \varepsilon_i}{\sum_{i=1}^{N} k_i}, \tag{8}$$

where the weights k_i are a function of the flow rate relative to the maximum flow rate

$$k_i = \begin{cases} \dfrac{Q_i}{Q_{max}}, & Q_i \leq 0.7 \cdot Q_{max} \\ 1.4 - \dfrac{Q_i}{Q_{max}}, & 0.7 \cdot Q_{max} < Q_i \leq Q_{max} \end{cases} \tag{9}$$

Where for mass-based meters Q_i is taken as per vendor specification (which may be volume or mass flow) and for volume-based meters the volume flow. The OIML also specifies the distribution of the test points among flow rates, however, in the case of sonic nozzles the possible flow rate distribution is fixed by the set of nozzle sizes.

The maximum permissible WME according to the OIML 137 classification is provided in Table 3. For CO_2 gas applications, an OIML class 1.5 would typically suffice. This means that both the MPE and WME should be within the limits provided in Table 1 and Table 3, respectively. Although DP-based devices are commonly not assessed according to OIML, the procedure as depicted in the OIML does provide a suitable structure to test these devices. The distinction between these different flow meter technologies originated mainly because of the different applications for oil and gas, and the expected uncertainty. For CO_2 applications, however, most meter technologies can comply with the current uncertainty demands of the industry.

Table 3 : WME specification from OIML 137 for type evaluation and initial verification

	Accuracy class		
	0.5	**1**	**1.5**
WME	±0.2 %	±0.4 %	±0.6 %

5 GENERAL RESULTS

5.1 Reference system

A cross-plot is used to visually compare and analyze the deviations between different measurement techniques used in the refrence system.
The cross-plot for the medium temperature test is provided in Figure 5-1, where the nitrogen is provided in blue, the 95 % CO_2 in light-grey, 98 % CO_2 in dark-grey and 99.5 % CO_2 in black; the different pressures are distinguished by the symbols. As observed, the 32 bara 99.5 % and 95 % CO_2 are not in the cross-plot due to the operation of the sonic nozzles near the phase boundary, leading to invalid sonic nozzle data. The 98 % CO_2 at 32 bara were intentionally run at a higher temperature, which causes the throat conditions of the nozzle to be within the region far from the phase boundary, leading to accurate sonic nozzle results.

The results obtained from the reference system indicate that the claimed uncertainties of the turbine and Coriolis reference system (as stated by PTB in [**7**]) still hold for a large part of the test data and can be used for the assessment of the meters under test in CO_2 conditions. For the medium temperature test, it was observed that the statistical spread of the turbine meters was larger than in previous JIPs. This is atypical for the reference system and further analysis showed that the flow conditioner upstream the turbine meters was partly blocked by small pieces of pipe coating. The estimated area blockage by these small pieces is estimated to be around 1 % of the total area of the flow conditioner. This led to a systematic offset and may also lead to worse reproducibility since these coating pieces were not fixed to the flow conditioner. Further investigation should be undertaken to fully understand the impact of the partially blocked flow conditioner. For the results of the medium temperature test, the offset of the turbine meters will be corrected by using the sonic nozzles as the reference. Also, for the medium temperature test the turbine meter uncertainty will be increased from the normal 0.25 % to 0.30 %.

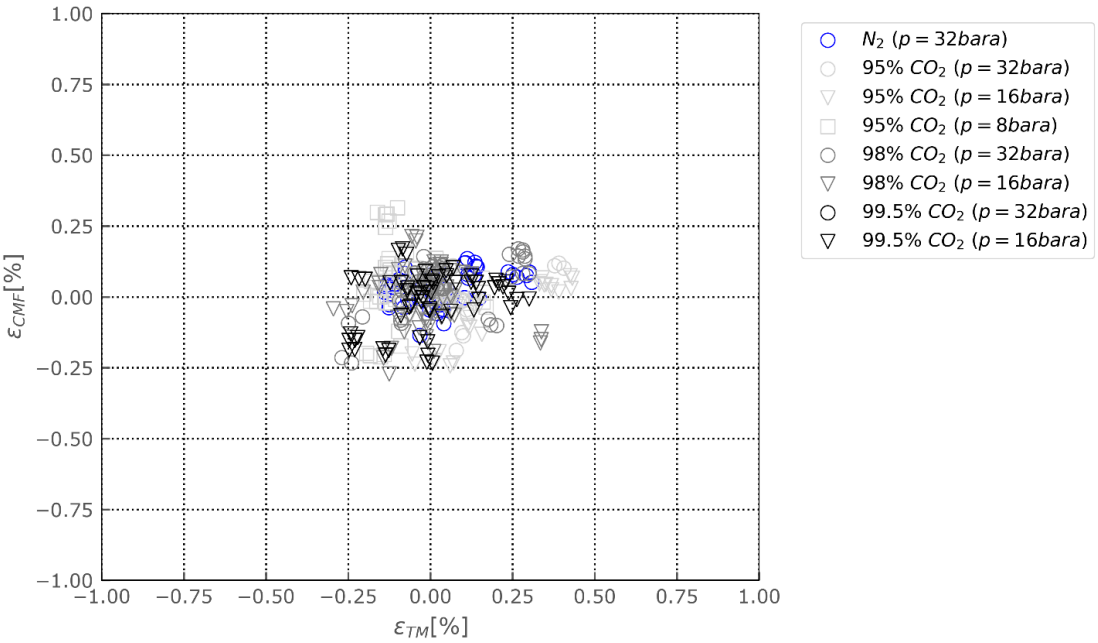

Figure 5-1 : Cross-plot of the turbine meter error versus the Coriolis meter error with reference based on the sonic nozzles

The cross-plot for the low temperature test is provided in Figure 5-2, where the nitrogen is provided in blue, and 99.5 % CO_2 in black; the different pressures are distinguished by the symbols. Also, in this cross-plot the turbine meters have a higher spread than expected, caused by a few test points. Inspection of the turbine meters showed that no obstructions were present

at the flow conditioner. The positive turbine meter outliers are at low flow rate and low pressure where the bearing friction correction becomes important. It is assumed that the temperature correction for the dynamic bearing friction coefficient as stipulated in equation (**3**) is overpredicted by the viscosity model and therefore leads to a positive offset for the turbine meters.

The results obtained from the reference system indicate that the claimed uncertainties of the turbine and Coriolis reference system (as stated by PTB in the JIP Renewable gases) still hold for the test data and can be used for the assessment of the meters under test in CO_2 conditions.

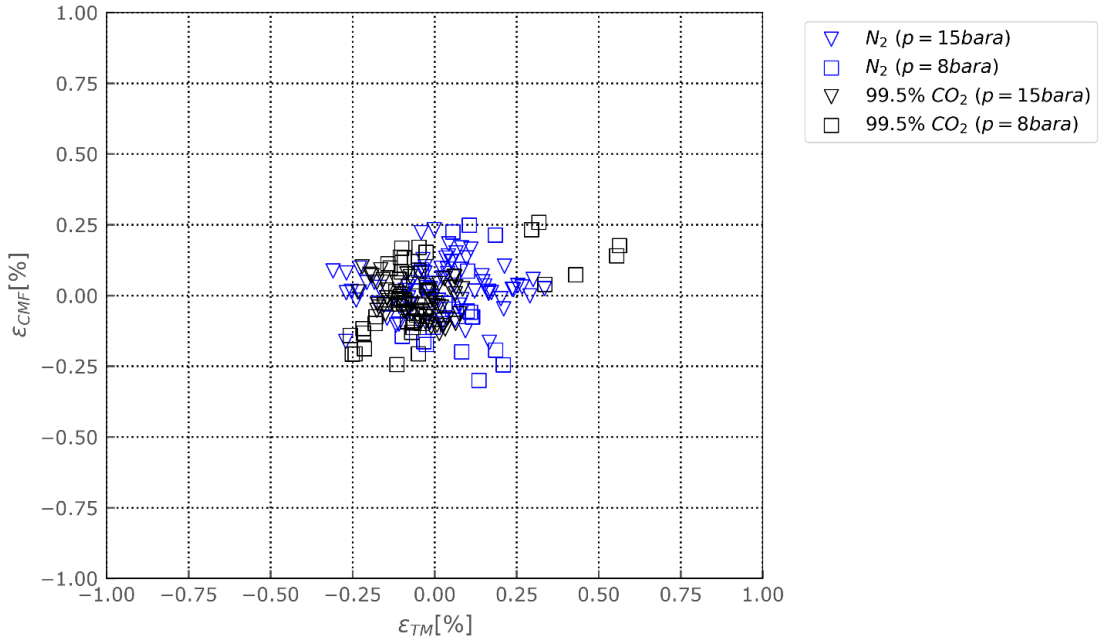

Figure 5-2 : Cross-plot of the turbine meter error versus the Coriolis meter error with reference based on the sonic nozzles

The total claimed expanded uncertainty (95 % confidence interval) of the flow reference system when all reference meters are in operation is:

$$U^*_{\mathrm{CMC}}(\dot{m}_{ref}) = 0.25\ \%. \tag{10}$$

For the total uncertainty of the mass flow rate also the stability of the test point itself is considered by means of the repeatability of the flow rates and density. This typically leads to an operational reference system uncertainty of approximately 0.3 %.

5.2 Meters Under Test results

The JIP covered the performance test of multiple metering technologies and multiple vendors for most metering technologies. This allows us to make general statements on the performance of these meters under gaseous CO_2 conditions without going into the details of specific meter vendors (as was done in [**9**]).

5.2.1 Coriolis meters

The response of the Coriolis meter group was generally consistent and demonstrated that these meters are insensitive to changes in gas composition and process conditions (given the meter is corrected for the pressure effect, see equation (**4**)). Depending on the size and drive frequency of the Coriolis meter, the meter should be compensated for the speed of sound, as

explained in equation (**5**). Since the speed of sound of CO_2 is relatively low this effect will become more dominant than for other gases.

Small WMEs of within 0.3 % were typically obtained and the resulting standard deviation for each test set was well within 0.3 % for all Coriolis meters. This resulted in a OIML classification of OIML class 0.5 or 1 for the Coriolis meters.

For the low temperature test, the behaviour of the Coriolis meters is largely identical. Since the zero-point of Coriolis meters is sensitive to stresses on the flanges, a difference in zero-point stability was expected for the low temperature test, since the larger temperature range induce larger pipe stresses. The results showed that this did not lead to a significantly larger zero-point effect compared to the medium temperature test above Q_t.

5.2.2 Ultrasonic meters

The response of the ultrasonic meters showed an inconclusive result. Some meters produced reproducible results between gas compositions and conditions and others did not. As explained in section 3.3, the DNV reference ultrasonic meter partly failed for the nitrogen baseline test on the top and bottom path measurements. It is expected that the higher speed of sound of nitrogen results in an increased beam width and cause reflection on the paths close to the wall. This indicates that the meter was specifically designed for CO_2 applications and that the performance on other gases is not necessarily representative for CO_2. Assuming transferability of calibration results between different gases is therefore not straight-forward and depends on the ultrasonic meter design.

For the CO_2 tests, the ultrasonic meters showed a very consistent Reynolds trend (differing in magnitude) and when compensated for this systematic trend the residual deviations are approximately +/-0.25 % from the Reynolds curve. It is expected that ultrasonic meters generally should be able to classify within OIML class 0.5 or 1 provided that the meter is calibrated on CO_2.

5.2.3 Differential pressure meters

To state a general conclusion on differential pressure devices is more difficult since the meters were not all correctly configured. The general behaviour of the DP meters showed that they follow a consistent Reynolds curve and therefore with correct physical properties the meter should be reproducible and consistent along all the test conditions. It is expected that when corrected for the systematic bias the differential pressure meters should be able to classify within OIML class 1 or 1.5 provided that the meter is calibrated on Reynolds number and has proper input for the physical properties of CO_2.

5.1.4 Vortex meters and turbine meters

Also vortex meters and a turbine meter were tested in the JIP CO_2MET Gas. Due to limited number of different vendors and to respect the agreed confidentiality no explicit statement will be made on the performance of the meters.

6 CONCLUSIONS

The active participation of industry stakeholders in Joint Industry Projects (JIPs) plays a crucial role in advancing knowledge and best practices. By engaging in JIPs, companies contribute valuable practical insights, share experiences, and help ensure that standards are both comprehensive and applicable to real-world scenarios. The proactive involvement of industry partners promotes the shared responsibility for quality and reliability of the knownlegde gained, ultimately driving advancements that benefit the entire industry ecosystem.

The JIP CO_2MET Gas has been a first step to enable technical developments and assess the current performance of gas flow measurement systems in CCUS transport networks. The general results presented in this paper are based on a minimum of 3 different vendors per technology and may therefore be deemed respresentative for the current state of the technology. Moreover, the results were consistent with the initial tests in 2021, see [**9**]. The performance results look promising since typically an OIML class of 1 is achievable which should suffice for the current requirements. Nevertheless, it is expected that vendors will further develop their technology for future demands in CCUS applications.

Looking ahead, new JIP CO2MET projects focused on liquid, dense and supercritical CO_2, as well as enhanced quality monitoring, will be essential in addressing the technical challenges of CCUS. The continued active participation of industry in these initiatives are important and shape the future of accurate and reliable flow measurement in CCUS systems.

7 NOTATION

$\boldsymbol{a_j}$ Reynolds curve coefficient
b_j Bearing friction coefficients
c Speed of sound
c_p Temperature correction factor
$\boldsymbol{d}$ Viscosity model coefficient for temperature
g Reynolds correction curve
$\boldsymbol{b_j}$ Bearing friction coefficients
p Pressure
T Temperature
Q Volume/mass flow rate
R Tube radius of Coriolis meter
ε Deviation of Meter Under Test to reference system
ϵ_p Pressure correction term Coriolis meters
ϵ_c Speed of sound correction term Coriolis meters
ω Angular tube frequency Coriolis meter
κ Isentropic exponent

References

[1] AGA, *Thermodynamic Properties of Natural Gas and Related Gases DETAIL and GROSS Equations of State*, Report No 8 Part 1(2017)
[2] Y. Alghanmi *et al.*, *Flow Meter Performance for The New Hydrogen and Carbon Capture Economy*, GFMW 2022.
[3] Emerson, *Micro Motion Elite Coriolis Flow and Density Meters: Product Data Sheet PS-00374*, Rev AK (2020)
[4] C. Hagenvik, D.S. van Putten and D. Maeland, *Exploring the relationship between speed of sound, density and isentropic exponent*, GFMW (2024)
[5] J. Hemp and J. Kutin, *Theory of errors in Coriolis flowmeter readings due to compressibility of the fluid being metered*, Flow Meas. Instr. 17 (2006)
[6] J. Gernert and R. Span, *EOS-CG: A Helmholtz energy mixture model for humid gases and CCS mixtures.* J. Chem. Thermodynamics 93 274-293 (2016); Herrig, S. *New Helmholtz-Energy Equations of State for Pure Fluids and CCS-Relevant Mixtures.* MSc Thesis. Fakultät für Maschinenbau der Ruhr-Universität Bochum (2018).
[7] J.G.M. van der Grinten, B. Mickan, H. Riezebos and D.S. van Putten, *Flowmeter traceability for non-conventional gases*, NSFMW 2021.
[8] OIML 137-1/2: *Gas meters Part 1: Metrological and technical requirements, Part 2: Metrological controls and performance tests* (2014)
[9] D.S. van Putten and R. Kruithof, *Flowmeter performance under CO_2 gaseous conditions*, NSFMW 2021.
[10] D.S van Putten, R. ten Cate, M. Al Saleem. *Considerations for CO2 metering and allocation systems*, GFMW 2023.